The ups and downs of ectoine: structural enzymology of a major microbial stress protectant and versatile nutrient

Lucas Hermann, Christopher-Nils Mais, Laura Czech, Sander H.J. Smits, Gert Bange and Erhard Bremer

Supplementary material

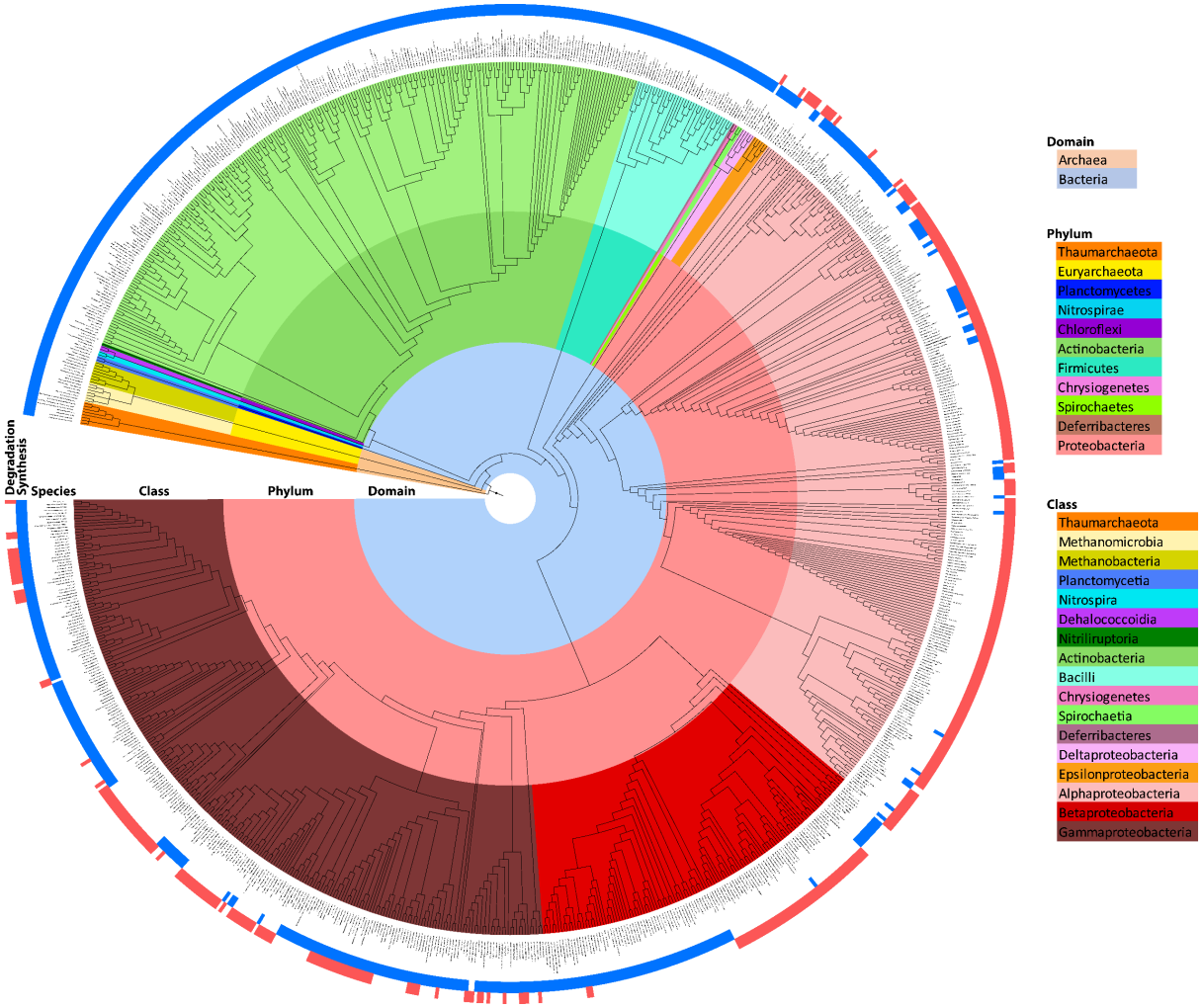

Supplementary Figure S1: Phylogenetic tree of microorganisms predicted to synthesize and/or to degrade ectoines.

Based on previous database searches by Czech et al. (2018) and Mais et al. (2020), fully sequenced genomes of *Bacteria* (8 557) and *Archaea* (293) deposited in the IMG/MER database (Chen et al., 2019) was searched from potential ectoine synthesizing microorganisms and those that are predicted to consume ectoine. The presence of gene (*ectC*) for the ectoine synthase (EctC) in the context of the other genes (*ectBA*) involved in ectoine synthesis (Czech et al., 2018) is marked with a blue square. The ability to degrade ectoines (Mais et al., 2020) was predicted by the co-adjacent genes for the ectoine utilization bi-module EutD/EutE, and is marked with a red square next to the respective microorganism. In this way, 676 microorganisms were predicted to synthesize ectoine, while 429 bacteria are predicted to consume ectoine. In this dataset, there are 96 microorganisms represented that are predicted to both synthesize and catabolize ectoine (Mais et al., 2020). A manually curated 16S rRNA-based phylogenetic tree was established by aligning the 16S rRNA DNA sequences with Clustal O (Sievers et al., 2011) and graphically represented with the iTOL tool (Letunic and Bork, 2016). Phylogenetic affiliations of microorganisms to domains, phyla and class are shown by color-code as listed in the figure.

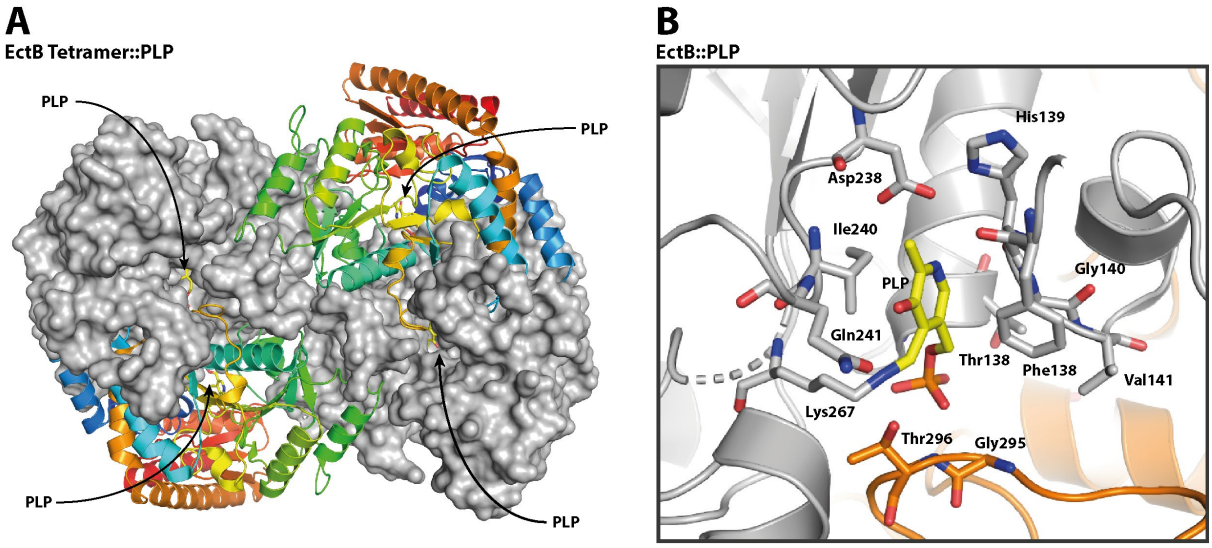

Supplementary Figure S2: Crystal structure of the L-2,4-diaminobutyrate transaminase EctB from *Chromohalobacter salexigens* in complex with pyridoxal-5'-phosphate (PLP).

Overview of the EctB tetramer with pyridoxal-5'-phosphate (PLP) bound in the active site of each monomer [PDB accession code: 6RL5] (Hillier et al., 2020). Two oft he EctB monomers are shown in cartoon representation with a rainbow coloring from carboxy-terminus to amino-terminus, while the two other monomers in the tetrameric assembly are depicted in surfaces representation modus. (B) Architecture of the active site of EctB with the covalently bound PLP (shown as yellow sticks) and amino acid residues highlights that are presumably involved in the enzyme reaction catalyzed by the EctB L-2,4-diaminobutyrate transaminase. Crystallographic data deposited in the PDB-file 6RL5 were used to render this cartoon using PyMol (Delano, 2002).

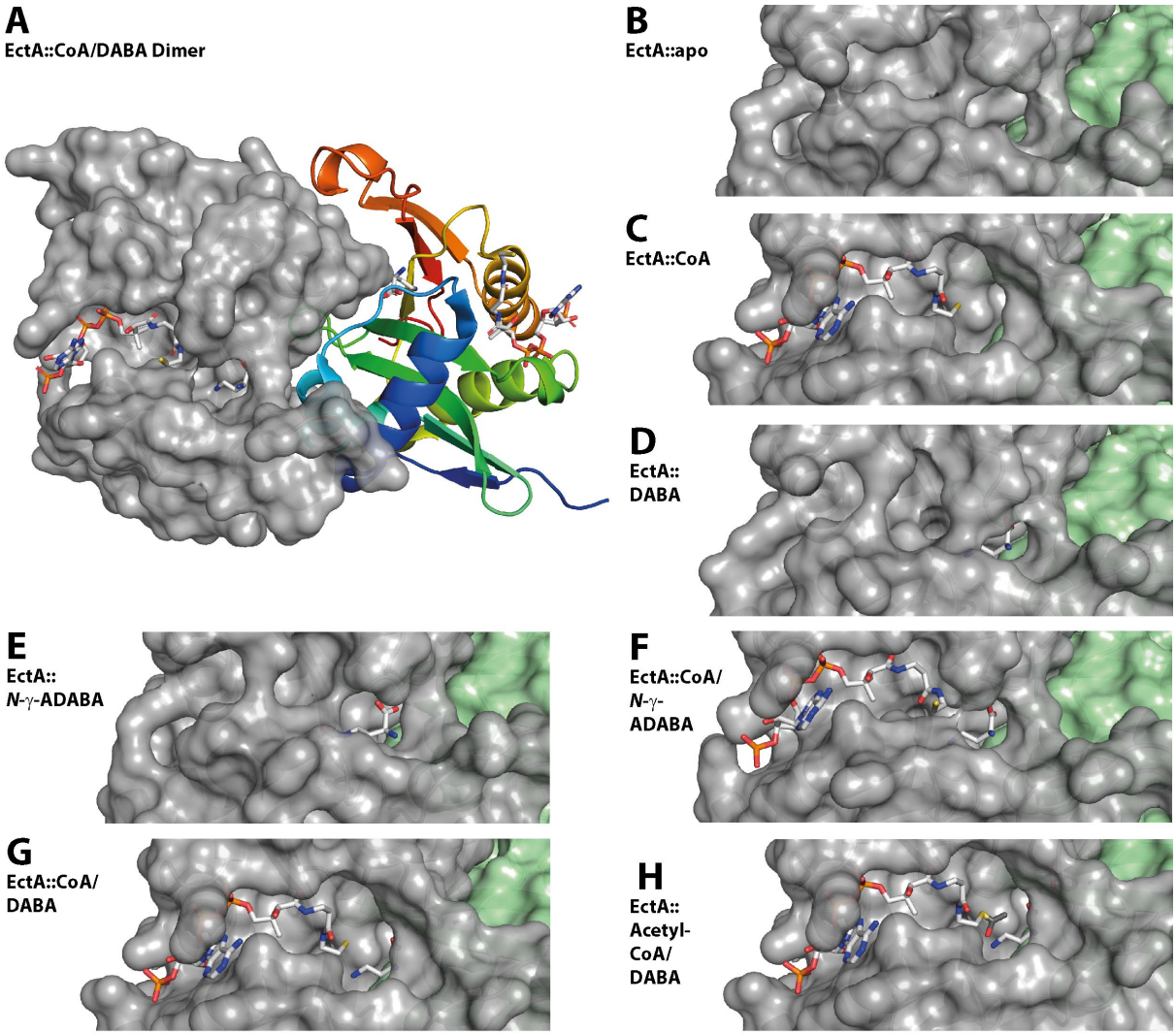

Supplementary Figure S3: A structural view of the reaction steps of the EctA diaminobuytrate acetyltransferase from *Paenibacillus lautus*.

This figure represents crystal structure of the EctA diaminobuytrate acetyltransferase from the thermotolerant bacterium *Paenibacillus lautus* in its apo, substrate- and enzyme reaction product-bound forms (Richter et al., 2020). (A) Overview of the EctA-dimer in complex with CoA and DABA [PDB accession code: 6SLL]. One of the monomers is shown in a cartoon representation with a rainbow coloring from carboxy-terminus to amino-terminus, while the second monomer is depicted in surfaces representation modus. (B) The empty binding sites for the substrates acetyl-CoA and DABA in the apo-form of EctA is shown [PDB accession code: 6SLK]. (C) Crystal structure of EctA in complex with CoA [PDB accession code: 6SK1]. (D) Crystal structure of EctA in complex with DABA [PDB accession code: 6SL8]. (E) Crystal structure of EctA in complex with γ-ADABA [PDB accession code: 6SJY]. (F) Crystal structure of EctA in complex with DABA and CoA [PDB accession code: 6SLL]. (G) γ-ADABA and CoA bound in the active sites of EctA [PDB accession code: 6SJY]. (H) Crystal structure of EctA in complex with DABA and CoA in which with an acetyl-group was added *in-silico* to the CoA sulfur to mimic the architecture of the EctA active site prior to enzyme catalysis. This picture

was generated by using the crystal structure of EctA in complex with DABA and CoA [PDB accession code: 6SLL] a the template. Crystallographic data deposited in the indicated PDB-files were used to render each cartoon by using PyMol (Delano, 2002). The depicted EctA dimers are depicted in surfaces representation modus; one monomer of EctA is depicted in grey, and the second monomer is depicted in green.

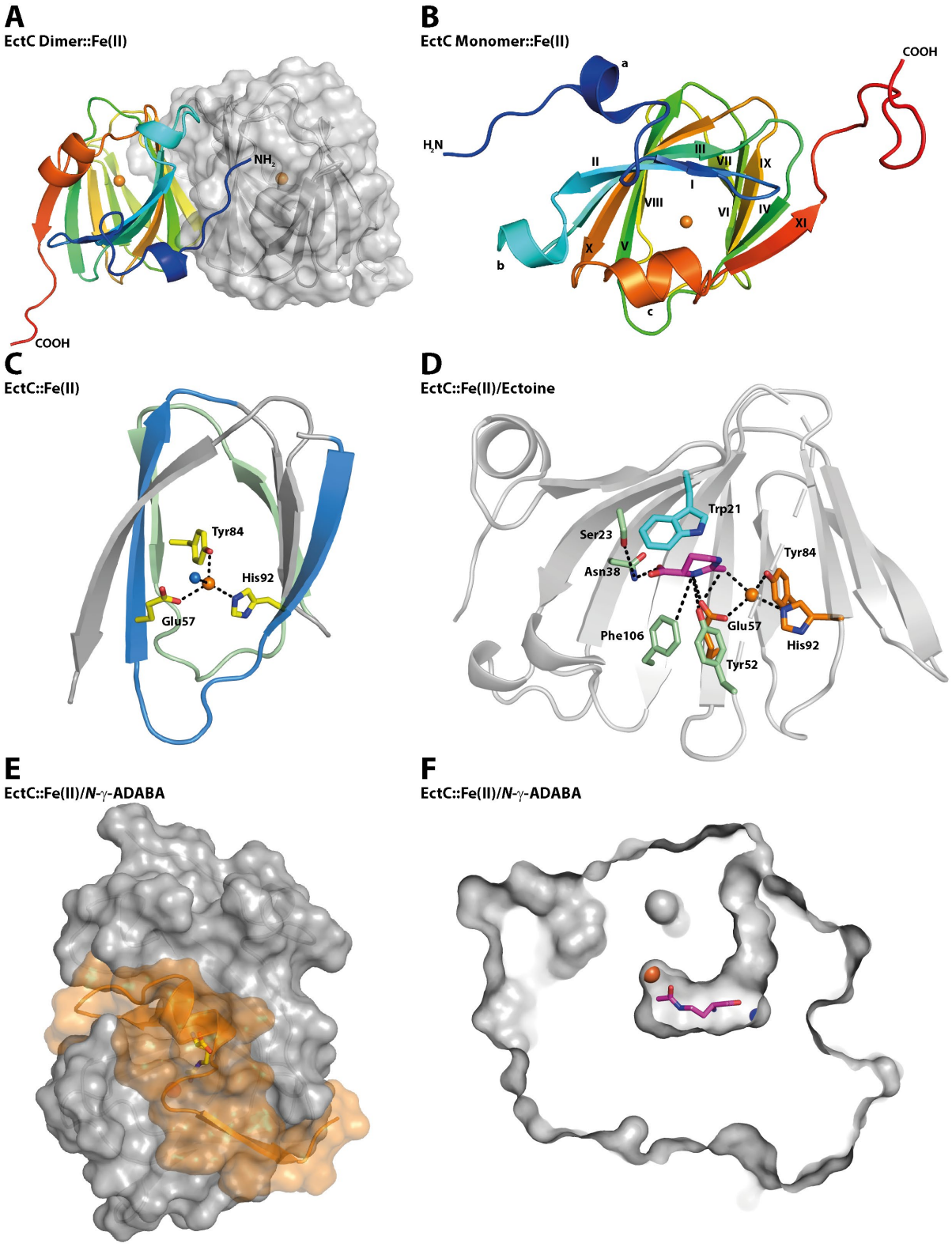

Supplementary Figure S4: Structural insights of the ectoine synthase EctC from *Paenibacillus lautus*. (A) The *Paenibacillus lautus* ectoine synthase (*Pl*EctC) (Czech et al., 2019) is a dimer present in a head-to-tail configuration with the iron catalyst (red sphere) bound in each monomer. The first monomer is shown in cartoon representation with a rainbow coloring from carboxy-terminus to amino-terminus, while the second monomer is depicted in surfaces representation modus [PDB accession code: 5ONM].

(B) The *Pl*EctC monomer in complex with iron is shown in a side-view with a rainbow-coloring from amino- to carboxy-terminus. The β-strands are labeled by roman numbers, and the three α-helices are marked by letters (a, b and c). (C) Close-up view of the iron-binding site of the *Pl*EctC protein (PDB code 5ONM). The iron (red sphere) is coordinated by the side-chains of Glu-57, Tyr-84, and His-92 and a localized water molecule (blue sphere); it has a distance of 2.9 Å to the iron atom. The two conserved cupin-motifs include those residues that coordinate the metal ion and are highlighted as part of the overall fold of the protein *Pl*EctC. (D) Iron (red sphere) and ectoine (gray sticks) bound in the catalytic core of the *Pl*EctC protein [PDB accession code: 5ONO]. The side-chains of the iron coordinating amino acids are depicted in orange, while the ectoine coordinating side-chains are shown in green. The side-chain of the catalytically relevant residue Trp-21 is shown in cyan. (E) Surface representation of the (*Pl*)EctC crystal structure with *N*-γ-ADABA [PDB accession code: 5ONN] in which the lid region (Czech et al., 2019; Widderich et al., 2016) is highlighted in orange; *N*-γ-ADABA is shown as yellow sticks and the iron atom is represented as a red sphere. (F) Cross-section through the catalytic core of the (*Pl*)EctC::Fe/*N*-γ-ADABA crystal structure [PDB accession code: 5ONN] with the entry tunnel for the *N*-γ-ADABA substrate. The positions of the catalytically important iron atom (red sphere) and a water molecule (blue sphere) are indicated. Crystallographic data deposited in the indicated PDB-files were used to render each cartoon by using PyMol (Delano, 2002).

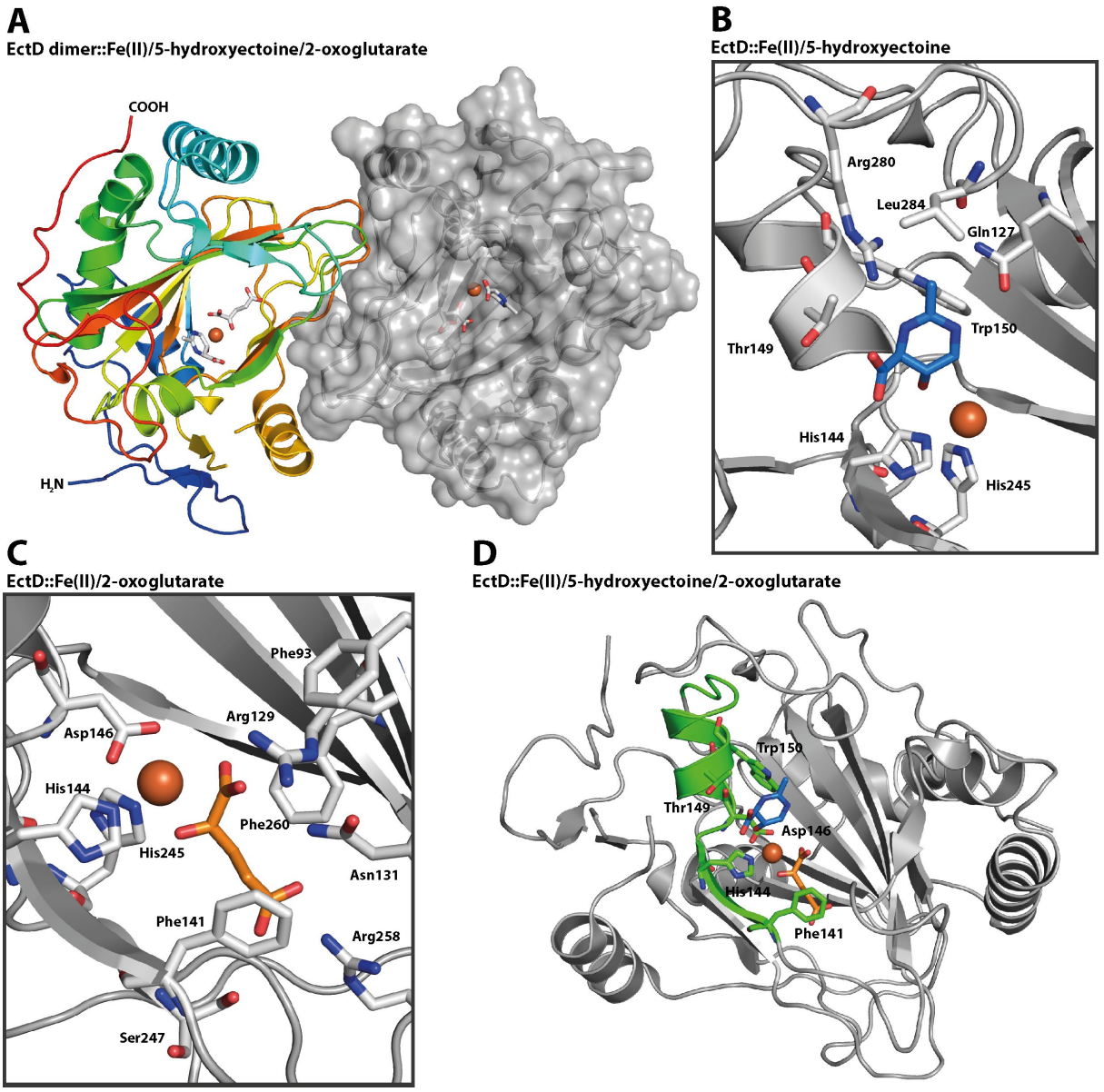

Supplementary Figure S5: Crystal structures of the ectoine hydroxylase EctD from *Sphingopyxis alaskensis*.

(A) Overview of the *Sphingopyxis alaskensis* (*Sa*) dimer. One monomer is shown in cartoon representation with a rainbow coloring from carboxy-terminus to amino-terminus while the second monomer is depicted in surfaces representation modus. Both Monomers have iron (orange sphere), 5-hydroxyectoine and 2-oxoglutarate bound in their active site [PDB accession code: 4Q5O]. (B) 5-hydroxyectoine (blue sticks) and iron (orange sphere) coordination in the catalytic center of the *Sa*EctD protein [PDB accession code: 4Q5O]. (C) 2-oxoglutarate (orange sticks) and iron (orange sphere) coordination in the catalytic center of the *Sa*EctD [PDB accession code: 4Q5O]. (D) The ectoine hydroxylase signature sequence motif (green) shown in the *Sa*EctD structure [PDB accession code: 4Q5O]. The side chains of the amino acids of the sequence motif coordinating ectoine (blue sticks), 2-oxogflutarate (orange sticks) and iron (orange sphere) are highlighted. Crystallographic data deposited

in the PDB-file 4Q5O (Höppner et al., 2014) were used to render each cartoon by using PyMol (Delano, 2002).

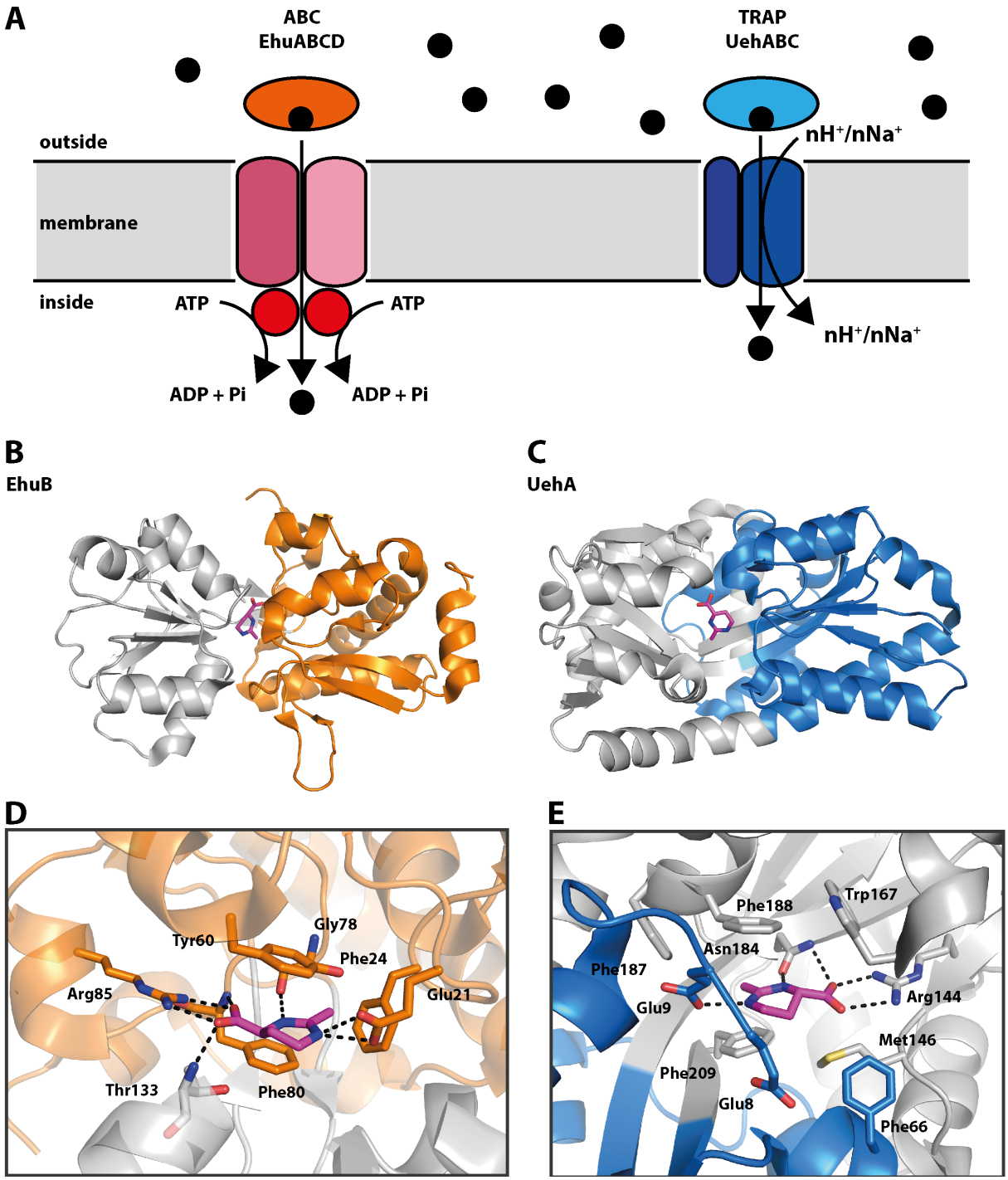

Supplementary Figure S6: ABC- and TRAP-type transporters used for the scavenging of ectoine and 5-hydroxyectoine when they are used as nutrients.

The EhuABCD system from *Sinorhizobium meliloti* is an ATP-binding-cassette (ABC) type transporter (Jebbar et al., 2005), while the UehABC system from *Ruegeria pomeroyi* is a member of the Tripartite ATP-independent periplasmic (TRAP) transporter family (Schulz et al., 2017b). The EhuB and UehA proteins are the extracellular substrate-binding proteins of these transporters; these have been crystalized in the presence of ectoine (Lecher et al., 2009; Hanekop et al., 2007). The transcription of the genes encoding the EhuABCD and UehABC importers is strongly induced when ectoine or 5-hydroxyectoine

is present in the growth medium, thereby reflecting the function of these transport systems for the acquisition of ectoines for use as nutrients (Jebbar et al., 2005; Schulz et al., 2017a; Lecher et al., 2009). (A) Schematic overview on the subunit composition of the EhuABCD and UehABC system. The transport activity of the Ehu transporter is fueled by ATP-hydrolysis, while that of the Ueh system is energized either by a proton (H^+) or a sodium (Na^+) gradient. (B and C) Overall fold of the EhuB [PDB accession code: 2Q88] (Hanekop et al., 2007) and UehA [PDB accession code: 3FXB] (Lecher et al., 2009) substrate binding proteins cyrstalized in the presence of ectoine. The two domains in EhuB and UehA are highlighted in grey/orange (B) and grey/blue (C), respectively. The bound ectoine ligand is shown as pink sticks. (D, E) Zoom into the ligand-binding site of EhuB (D) and UehA (E) and. All residues involved in ectoine binding are depicted as sticks; the ectoine ligand is shown in pink sticks. Crystallographic data deposited in the indicated PDB-files were used to render each cartoon by using PyMol (Delano, 2002).

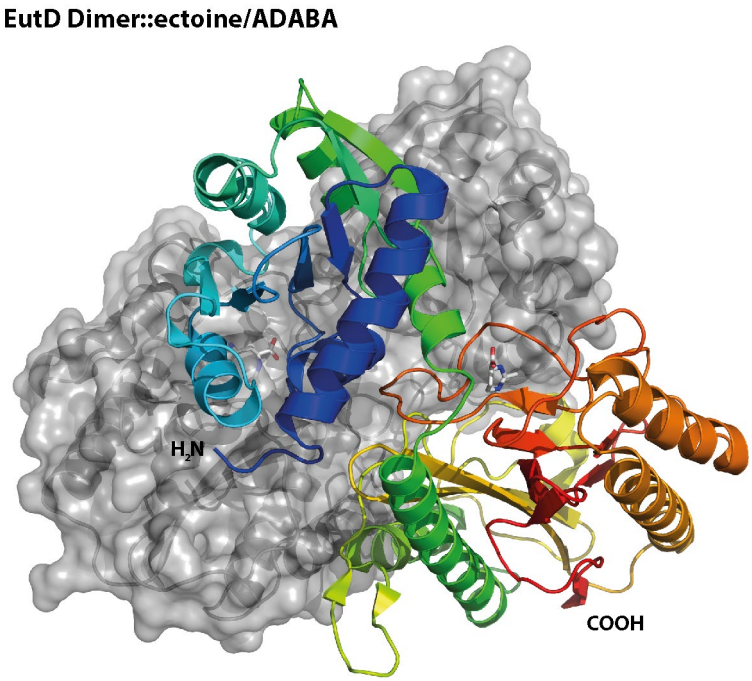

Supplementary Figure S7: Overview of the dimer of the ectoine/5-hydroxyectoine hydrolase EutD from *Halomonas elongata* [PDB accession code: 6TWK]. Monomer_1 is shown in cartoon representation with a rainbow coloring from the carboxy-terminus to the amino-terminus while monomer_2 is depicted in surfaces representation modus. In the active site of monomer I the substrate, ectoine, of the enzyme is bound, while in the active site of monomer II the reaction product, *N*-α-ADABA, of the ectoine hydrolase is present (Mais et al., 2020). Crystallographic data deposited in the indicated PDB-file were used to render each cartoon by using PyMol (Delano, 2002).

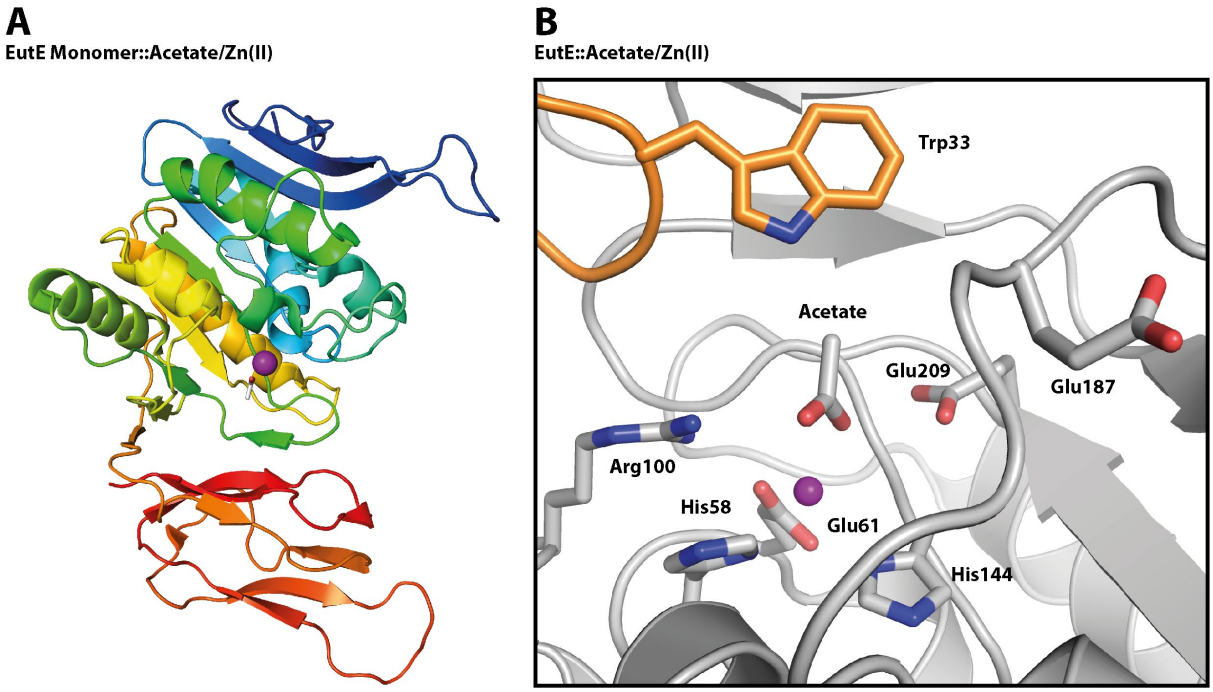

Supplementary Figure S8: Structural overviews of the *N*-α-ADABA deacetylase EutE from *Ruegeria pomeroyi.*

(A) The EutE protein is a *N*-acetyl-diaminobutyrate deacetylase (Mais et al., 2020). An overview of the monomeric *Ruegeria pomeroyi* (*Rp*) EutE protein is shown in cartoon representation with a rainbow coloring from carboxy-terminus to amino-terminus. In this crystal structure, the catalytically critical zinc ion (purple sphere) and the reaction product, acetate (sticks), of the (*Rp*)EutE protein is present in the active site [PDB accession code: 6TWM] (Mais et al., 2020). (B) A view into the active site of the (*Rp*)EutE protein with bound zinc (purple sphere) and acetate (sticks) [PDB accession code: 6TWM]. Crystallographic data deposited in the indicated PDB-file were used to render each cartoon by using PyMol (Delano, 2002).

References

Chen, I.A., Chu, K., Palaniappan, K., Pillay, M., Ratner, A., Huang, J., Huntemann, M., Varghese, N., White, J.R., Seshadri, R., Smirnova, T., Kirton, E., Jungbluth, S.P., Woyke, T., Eloe-Fadrosh, E.A., Ivanova, N.N. and Kyrpides, N.C. (2019). IMG/M v.5.0: an integrated data management and comparative analysis system for microbial genomes and microbiomes. Nucleic Acids Res. *47*, D666-D677.

Czech, L., Hermann, L., Stöveken, N., Richter, A.A., Höppner, A., Smits, S.H.J., Heider, J. and Bremer, E. (2018). Role of the extremolytes ectoine and hydroxyectoine as stress protectants and nutrients: genetics, phylogenomics, biochemistry, and structural analysis. Genes (Basel) *9*, 177.

Czech, L., Höppner, A., Kobus, S., Seubert, A., Riclea, R., Dickschat, J.S., Heider, J., Smits, S.H.J. and Bremer, E. (2019). Illuminating the catalytic core of ectoine synthase through structural and biochemical analysis. Sci. Rep. *9*, 364.

Delano, W.L. (2002). The *PyMol* molecular graphics system. Delano Scientific, San Carlos, CA, USA.

Hanekop, N., Höing, M., Sohn-Bösser, L., Jebbar, M., Schmitt, L. and Bremer, E. (2007). Crystal structure of the ligand-binding protein EhuB from *Sinorhizobium meliloti* reveals substrate recognition of the compatible solutes ectoine and hydroxyectoine. J. Mol. Biol. *374*, 1237-1250.

Hillier, H.T., Altermark, B. and Leiros, I. (2020). The crystal structure of the tetrameric DABA-aminotransferase EctB, a rate-limiting enzyme in the ectoine biosynthesis pathway. FEBS J., (in press) (doi: 10.1111/febs. 15265).

Höppner, A., Widderich, N., Lenders, M., Bremer, E. and Smits, S.H.J. (2014). Crystal structure of the ectoine hydroxylase, a snapshot of the active site. J. Biol. Chem. *289*, 29570-29583.

Jebbar, M., Sohn-Bösser, L., Bremer, E., Bernard, T. and Blanco, C. (2005). Ectoine-induced proteins in *Sinorhizobium meliloti* include an ectoine ABC-type transporter involved in osmoprotection and ectoine catabolism. J. Bacteriol. *187*, 1293-1304.

Lecher, J., Pittelkow, M., Zobel, S., Bursy, J., Bonig, T., Smits, S.H., Schmitt, L. and Bremer, E. (2009). The crystal structure of UehA in complex with ectoine-A comparison with other TRAP-T binding proteins. J. Mol. Biol. *389*, 58-73.

Letunic, I. and Bork, P. (2016). Interactive tree of life (iTOL) v3: an online tool for the display and annotation of phylogenetic and other trees. Nucleic Acids Res. *44*, W242-W245.

Mais, C.-N., Hermann, L., Altegoer, F., Seubert, A., Richter, A.A., Wernersbach, I., Czech, L., Bremer, E. and Bange, G. (2020). Degradation of the microbial stress protectants and chemical chaperones ectoine and hydroxyectoine by a bacterial hydrolase-deacetylase complex. J. Biol. Chem. (in press) (doi: 10.1074/jbc.RA 120.012722).

Richter, A.A., Kobus, S., Czech, L., Hoeppner, A., Zarzycki, J., Erb, T.J., Lauterbach, L., Dickschat, J.S., Bremer, E. and Smits, S.H.J. (2020). The architecture of the diaminobutyrate acetyltransferase active site provides mechanistic insight into the biosynthesis of the chemical chaperone ectoine. J. Biol. Chem. *295*, 2822-2838.

Schulz, A., Hermann, L., Freibert, S.-A., Bönig, T., Hoffmann, T., Riclea, R., Dickschat, J.S., Heider, J. and Bremer, E. (2017a). Transcriptional regulation of ectoine catabolism in response to multiple metabolic and environmental cues. Env. Microbiol. *19*, 4599-4619.

Schulz, A., Stöveken, N., Binzen, I.M., Hoffmann, T., Heider, J. and Bremer, E. (2017b). Feeding on compatible solutes: a substrate-induced pathway for uptake and catabolism of ectoines and its genetic control by EnuR. Environ. Microbiol. *19*, 926-946.

Sievers, F., Wilm, A., Dineen, D., Gibson, T.J., Karplus, K., Li, W., Lopez, R., McWilliam, H., Remmert, M., Soding, J., Thompson, J.D. and Higgins, D.G. (2011). Fast, scalable generation of high-quality protein multiple sequence alignments using Clustal Omega. Mol. Syst. Biol. *7*, 539.

Widderich, N., Kobus, S., Höppner, A., Ricela, R., Seubert, A., Dickschat, J.S., Heider, J., Smits, S.H.J. and Bremer, E. (2016). Biochemistry and crystal structure of the ectoine synthase: a metal-containing member of the cupin superfamily. PLoS One *11*, e0151285.